Cardiovascular Research (2009) **81**, 686–694
doi:10.1093/cvr/cvn339

A transient outward potassium current activator recapitulates the electrocardiographic manifestations of Brugada syndrome

Kirstine Calloe[1*†], Jonathan M. Cordeiro[2†], José M. Di Diego[2], Rie S. Hansen[3], Morten Grunnet[1,3], Søren Peter Olesen[1], and Charles Antzelevitch[2]

[1]*The Danish National Research Foundation Centre for Cardiac Arrhythmia, Department of Biomedical Sciences 12.5.10, University of Copenhagen, Blegdamsvej 3, DK-2200 Copenhagen N, Denmark;* [2]*Masonic Medical Research Laboratory, Utica, NY, USA; and* [3]*NeuroSearch A/S, Ballerup, Denmark*

Received 19 September 2008; revised 1 December 2008; accepted 4 December 2008; online publish-ahead-of-print 10 December 2008

Time for primary review: 17 days

KEYWORDS
Transient outward potassium current;
Ito;
Brugada syndrome;
Re-entry;
Arrhythmia

Aims Transient outward potassium current (I_{to}) is thought to be central to the pathogenesis of the Brugada syndrome (BrS). However, an I_{to} activator has not been available with which to validate this hypothesis. Here, we provide a direct test of the hypothesis using a novel I_{to} activator, NS5806.
Methods and results Isolated canine ventricular myocytes and coronary-perfused wedge preparations were used. Whole-cell patch-clamp studies showed that NS5806 (10 μM) increased peak I_{to} at +40 mV by 79 ± 4% (24.5 ± 2.2 to 43.6 ± 3.4 pA/pF, $n = 7$) and slowed the time constant of inactivation from 12.6 ± 3.2 to 20.3 ± 2.9 ms ($n = 7$). The total charge carried by I_{to} increased by 186% (from 363.9 ± 40.0 to 1042.0 ± 103.5 pA·ms/pF, $n = 7$). In ventricular wedge preparations, NS5806 increased phase 1 and notch amplitude of the action potential in the epicardium, but not in the endocardium, and accentuated the ECG J-wave, leading to the development of phase 2 re-entry and polymorphic ventricular tachycardia ($n = 9$). Although sodium and calcium channel blockers are capable of inducing BrS only in right ventricular (RV) wedge preparations, the I_{to} activator was able to induce the phenotype in wedges from both ventricles. NS5806 induced BrS in 4/6 right and 2/10 left ventricular wedge preparations.
Conclusion The I_{to} activator NS5806 recapitulates the electrographic and arrhythmic manifestation of BrS, providing evidence in support of its pivotal role in the genesis of the disease. Our findings also suggest that a genetic defect leading to a gain of function of I_{to} could explain variants of BrS, in which ST-segment elevation or J-waves are evident in both right and left ECG leads.

1. Introduction

Brugada syndrome (BrS) is an inherited disease associated with phase 2 re-entry, polymorphic ventricular tachycardia (PVT), and sudden cardiac death in young adults with a structurally normal heart. The ECG pattern of BrS is often concealed, but can be unmasked or modulated by fever, vagal stimulation, and a number of pharmacological agents.[1] BrS has been linked to decreased inward currents or increased outward currents during phase 1, accentuating the spike-and-dome morphology of the action potential (AP) mainly in the epicardium.[1] The transmural voltage gradient that develops gives rise to the characteristic ECG changes, consisting of a down-sloping ST-segment elevation or accentuated J-wave with a negative T-wave. In most cases, these ECG changes manifest principally in the right precordial leads,[2] although BrS cases of left precordial and inferior lead ST-segment elevations have been reported.[3–5] ST-segment elevation is often accompanied by QT prolongation in the right precordial leads, due to accentuation of the epicardial AP notch.[6]

On a molecular level, BrS has been linked to mutations in the *SCN5A* gene[7] encoding the $Na_v1.5$ channel α-subunit, in *SCN1B*[8] encoding the sodium channel β1-subunit, in the *glycerol-3-phosphate dehydrogenase 1 like gene* (*GPD1-L*),[9] as well as in mutations in the *CACNA1c* and *CACNB2b* genes[6] encoding the α1 and β2b subunits of the L-type calcium channel, respectively. Mutations in *SCN5A*, *SCN1B*, and *GPD1-L* all reduced peak sodium channel current (I_{Na}), whereas mutations in *CACNA1c* and *CACNB2b* led to a decrease in L-type calcium channel current. More recently, a mutation in the *KCNE3* gene resulting in increased I_{to} current has been associated with BrS.[10] Although a direct

* Corresponding author. Tel: +45 3532 7134; fax: +45 3532 7555.
E-mail address: kirstinec@mfi.ku.dk
†These authors contributed equally to this work.

link to I_{to} has only recently been established, I_{to} has long been thought to be central to the pathogenesis of BrS.[1] The presence of a prominent I_{to} predisposes the myocardium to the development of a BrS phenotype by amplifying phase 1 of the AP, thus leading to augmentation of the notched appearance of the AP, most notably in the RV epicardium. I_{to} is larger in the RV than in the left ventricle (LV),[11] accounting for the appearance of ST-segment elevation in the right precordial leads. Furthermore, BrS is more prevalent in males than in females, due at least in part to the presence of a more prominent I_{to} in RV of males.[12]

The present study examines the characteristics of a novel and unique I_{to} activator, NS5806, in isolated canine ventricular myocytes and wedge preparations. NS5806 is shown to recapitulate the electrocardiographic and arrhythmic manifestations of BrS, providing further evidence in support of its pivotal role in the genesis of the disease. Our findings also suggest that a genetic defect leading to a prominent gain of function of I_{to} could explain variants of BrS, in which ST-segment elevation or J-waves are evident in both right and left ECG leads.

2. Methods

2.1 NS5806

NS5806 was synthesized at NeuroSearch A/S, Ballerup, Denmark by reaction of 6-cyano-2,4-dibromoaniline with sodium azide to form the respective 2,4-dibromo-6-tetrazolylaniline, which was condensed with 3,5-bis-trifluoromethyl-phenylisocyanate to provide the target 1-[2,4-dibromo-6-(1H-tetrazol-5-yl)-phenyl]-3-(3,5-bis-trifluoromethyl-phenyl)-urea (NS5806). NS5806 was dissolved in dimethyl sulphoxide (20 mM stock).

2.2 Experimental animals

This investigation conforms to the Guide for Care and Use of Laboratory Animals published by the National Institutes of Health (NIH publication no. 85-23, Revised 1996). Adult mongrel dogs of either sex were anticoagulated with heparin and anaesthetized with pentobarbital (30–35 mg/kg, i.v.). Their hearts were rapidly removed and placed in a 4°C cardioplegic solution (in mM): NaCl 129, KCl 12, NaH_2PO_4 0.9, $NaHCO_3$ 20, $CaCl_2$ 1.8, $MgSO_4$ 0.5, and glucose 5.5.

2.3 Isolation of adult canine cardiomyocytes

Myocytes from the mid-myocardial (mid) region were prepared from canine hearts using techniques previously described.[13,14] A wedge consisting of the LV free wall supplied by a descending branch of the circumflex artery was excised, cannulated, and perfused with nominally Ca^{2+}-free solution (mM): NaCl 129, KCl 5.4, $MgSO_4$ 2.0, NaH_2PO_4 0.9, glucose 5.5, $NaHCO_3$ 20, bubbled with 95% O_2/5% CO_2 containing 0.1% bovine serum albumin (BSA) for a period of ~5 min. The wedge preparation was then subjected to enzyme digestion with the nominally Ca^{2+}-free solution supplemented with 0.5 mg/mL collagenase (Type II, Worthington), 0.1 mg/mL protease (Type XIV, Sigma), and 1 mg/mL BSA for 8–12 min. After perfusion, thin slices of tissue from the mid-region (about 5–7 mm from the epicardial surface) were shaved from the wedge using a dermatome. The tissue slices were then placed in separate beakers, minced, incubated in fresh buffer containing 0.5 mg/mL collagenase and 1 mg/mL BSA, and agitated. The supernatant was filtered, centrifuged at 200 rpm for 2 min, and the myocyte-containing pellet was stored in 0.5 mM Ca^{2+} HEPES buffer at room temperature.

2.4 Voltage-clamp recordings

Voltage-clamp and current-clamp recordings were made using a MultiClamp 700A amplifier and a MultiClamp Commander (Axon Instruments). Patch pipettes were fabricated from borosilicate glass capillaries (1.5 mm OD, Fisher Scientific, Pittsburgh, PA, USA) using a gravity puller (Model PP-830, Narishige, Tokyo, Japan), and the pipette resistance ranged from 1 to 3 MΩ. Cell capacitance was measured by integrating the current after applying −5 mV voltage steps. Electronic compensation of series resistance to 60–70% was applied to minimize voltage errors. All analogue signals (cell current and voltage) were acquired at 10–50 kHz, filtered at 4–6 kHz, digitized with a Digidata 1322 converter (Axon Instruments), and stored using pClamp9 software.

I_{to} recordings were performed, as described previously.[15] Initially, the ventricular cells were superfused with a HEPES buffer of the following composition (mM): NaCl 126, KCl 5.4, $MgCl_2$ 1.0, $CaCl_2$ 2.0, HEPES 10, glucose 11, pH 7.4. The patch pipette solution had the following composition (mM): K-aspartate 90, KCl 30, glucose 5.5, $MgCl_2$ 1.0, EGTA 5, MgATP 5, HEPES 5, NaCl 10, pH 7.2. The APs were recorded in this solution. For I_{to}, I_{K1}, and I_{Kr} measurements, the HEPES buffer was supplemented with 300 μM cadmium to block I_{Ca}, and for I_{Kr} measurements, 100 nM HMR1556 was present to block I_{Ks}. For I_{CaL} measurements, 5 mM TEA was added to the pipette solution to block potassium currents and cadmium was not added to the HEPES buffer.

Sodium currents were recorded, as described previously,[16] in a low Na^+ extracellular solution (mM): $CaCl_2$ 0.5, glucose 10, $MgCl_2$ 1.5, choline-Cl 120, NaCl 5, HEPES 10, KCl 4, Na acetate 2.8, $CoCl_2$ 1, $BaCl_2$ 0.1, pH 7.4. The pipette solution consisted of $MgCl_2$ 1, NaCl 15, KCl 5, CsF 120, HEPES 10, EGTA 10, Na_2ATP 4, pH 7.2. All experiments were performed at 37°C, except for the sodium current recordings which were performed at room temperature.

2.5 Wedge preparations of the free wall from right and left ventricles

Transmural wedges were dissected from the base of the RV (2 × 1.5 × 0.9 cm) and LV (3 × 2 × 1.5 cm). The preparations were initially arterially perfused with cardioplegic solution. Subsequently, the wedge preparations were placed in a tissue bath, perfused with Tyrode's solution (mM): NaCl 129, KCl 4, NaH_2PO_4 0.9, $NaHCO_3$ 20, $CaCl_2$ 1.8, $MgSO_4$ 0.5, glucose 5.5, pH 7.4, and bubbled with 95% O_2 and 5% CO_2 (37 ± 0.5°C). The perfusate was delivered at a constant flow at 8–11 mL/min, depending on the size of the wedge and the pressure was monitored throughout the experiment (*Table 1*). Pacing stimuli was delivered to the endocardial surface at two times the diastolic threshold of excitation (DTE). In all experiments, recordings were made at basic cycle lengths (BCLs) of 300, 500, 800, and 2000. Unless otherwise indicated, recordings at 2000 ms BCL are shown. The DTE was not affected by NS5806 (*Table 1*). Recordings were obtained after >1 h after mounting for control and 30 min after application of NS5806. A transmural pseudo-ECG (ECG) was recorded using two Ag/AgCl half cells placed at ~1 cm from the epicardial (+) and endocardial (−) surfaces of the preparation. Intracellular recordings were obtained simultaneously from the subendocardium (endo, ~2–3 mm from the endocardial surface) and from the subepicardium (epi, ~0–3 mm from the epicardial surface), using floating glass microelectrodes. ECG and AP signals were amplified and/or digitized and analysed using Spike 2 for Windows (Cambridge Electronic Design, Cambridge, UK).

2.6 Statistical analysis

Results are presented as mean ± SEM throughout the publication. Statistical comparisons were made using one-way analysis of variance and Dunnett's post test, unless otherwise indicated.

Table 1 Basic parameters measured in canine ventricular wedge preparations

NS5806 (μM)	LV transmural conduction time (ms)	RV transmural conduction time (ms)	ERP RV and LV (ms)	DTE RV and LV (mA)	Pressure (dia) RV (mmHg)	Pressure (sys) RV (mmHg)
0	15.0 ± 1.6, $n = 8$	13.7 ± 2.0, $n = 8$	196.7 ± 6.5, $n = 12$	0.81 ± 0.08, $n = 12$	49.1 ± 10.9, $n = 6$	58.2 ± 12.1, $n = 6$
5	15.3 ± 1.6, $n = 7$	12.1 ± 2.8, $n = 6$	198.9 ± 8.41, $n = 9$	0.96 ± 0.13, $n = 9$	45.7 ± 14.5, $n = 3$	53.5 ± 15.9, $n = 3$
10	13.0 ± 1.6, $n = 5$	14.5 ± 1.6, $n = 7$	218.3 ± 11.9, $n = 6$	0.84 ± 0.12, $n = 7$	62.8 ± 14.8, $n = 6$	70.4 ± 15.7, $n = 6$
15	22.1 ± 2.2, $n = 5$*	14.0 ± 3.7, $n = 4$	–	–	–	–
		NS	NS	NS	NS	NS

All parameters were measured at a BCL of 2000 ms. The conduction time was calculated as the time between the mid-point of phase 0 in the epicardium and endocardium. The diastolic threshold of excitation (DTE) was determined by increasing the injected current until capture. The refractory period (ERP) was measured by delivering premature stimuli at progressively shorter S1–S2 intervals after every 10th basic beat applied at a BCL of 2000 ms and at 1.5× DTE. The flow was kept constant between 8–11 mL/min and the pressure was measured. *$p < 0.05$ versus control.

3. Results

The molecular structure of NS5806 is shown in *Figure 1A*. *Figure 1B–F* illustrates the effect of NS5806 on APs and I_{to} recorded from myocytes isolated from the mid-region of the canine LV. At a cycle length of 1 s, the AP recorded under control conditions exhibited a prominent phase 1 repolarization, resulting in a spike-and-dome morphology. The application of 10 μM NS5806 increased phase 1, leading to loss of the AP dome when phase 1 reached potentials more negative than the threshold for the activation of the L-type calcium current, I_{CaL} (*Figure 1B*). Loss of the dome was accompanied by a significant abbreviation of the APD_{90}, from 372 ± 29.4 to 51.3 ± 18.7 ms ($n = 5$, $P < 0.05$). NS5806 (10 μM) reduced the maximal upstroke velocity of phase 0 (V_{max}) by 9.8 ± 3.4% (from 407.2 ± 34.4 to 367.0 ± 32.7 V/s, $n = 5$, $P < 0.05$); the amplitude of phase 0 was unaffected (121.6 ± 1.1 mV in control vs.120.3 ± 0.25 mV with NS5806, $n = 5$). The concentration of NS5806 was based on preliminary experiments in CHO-K1 cells expressing Kv4.3 and KChiP2, where we found an EC50 value of 7 μM.

The effect on the phase 1 repolarization suggested that I_{to} was increased by NS5806. As a test of this hypothesis, we recorded I_{to} in mid-myocardial cells using whole-cell patch-clamp techniques (*Figure 1C–G*). NS5806 (10 μM) significantly increased the magnitude of I_{to} at all potentials greater than −30 mV (*Figure 1D*). Inactivation was significantly slowed, as reflected by an increase in time constant (τ, from 12.6 ± 3.2 to 20.3 ± 2.9 ms at +40 mV, $n = 7$, $P < 0.05$; *Figure 1E*). The increased I_{to} peak-current amplitude together with the slowed inactivation resulted in a near three-fold increase in total charge, as reflected by an increase in area under the curve from 363.9 ± 40.0 to 1042 ± 103.5 pA·ms/pF at +40 mV ($n = 7$, $P < 0.05$; *Figure 1F*). The effects of the drug were fully reversed upon washout. Furthermore, the recovery from inactivation of I_{to} was faster in the presence of NS5806 (10 μM), as shown in *Figure 1G*.

We also examined the effect of NS5806 on other currents known to contribute to the development of the BrS phenotype. NS5806 (10 μM) caused a minor reduction in both I_{Na} and I_{CaL}, as shown in *Figure 2A* and *B*. As it has recently been suggested that the fast component of the delayed rectifier current I_{Kr} can contribute to BrS in humans[17] and an I_{Kr} agonist that modulates ERG channels resulting in I_{to}-like currents has been reported,[18] we assessed the effect of NS5806 on I_{Kr} in isolated endocardial myocytes. Endocardial cells were chosen to minimize the impact of I_{to}. We found that NS5806 (10 μM) caused a minor reduction in I_{Kr}, as shown in *Figure 2C*. We found no effect of NS5806 on I_{K1} (*Figure 2D*).

We next assessed the effect of increased I_{to} on the development of a BrS phenotype using canine ventricular wedge preparations. *Figure 3A* shows a representative example of the effect of NS5806 (5–15 μM) in an RV wedge preparation. Increasing the concentration of NS5806 caused a progressive increase in the epicardial phase 1 magnitude, whereas the APs of endocardial cells were largely unaffected. The increase in the epicardial notch magnitude was accompanied by an accentuation of the J-wave, or an apparent ST-segment elevation, on the ECG. The attending delay in epicardial repolarization led to the reversal of the

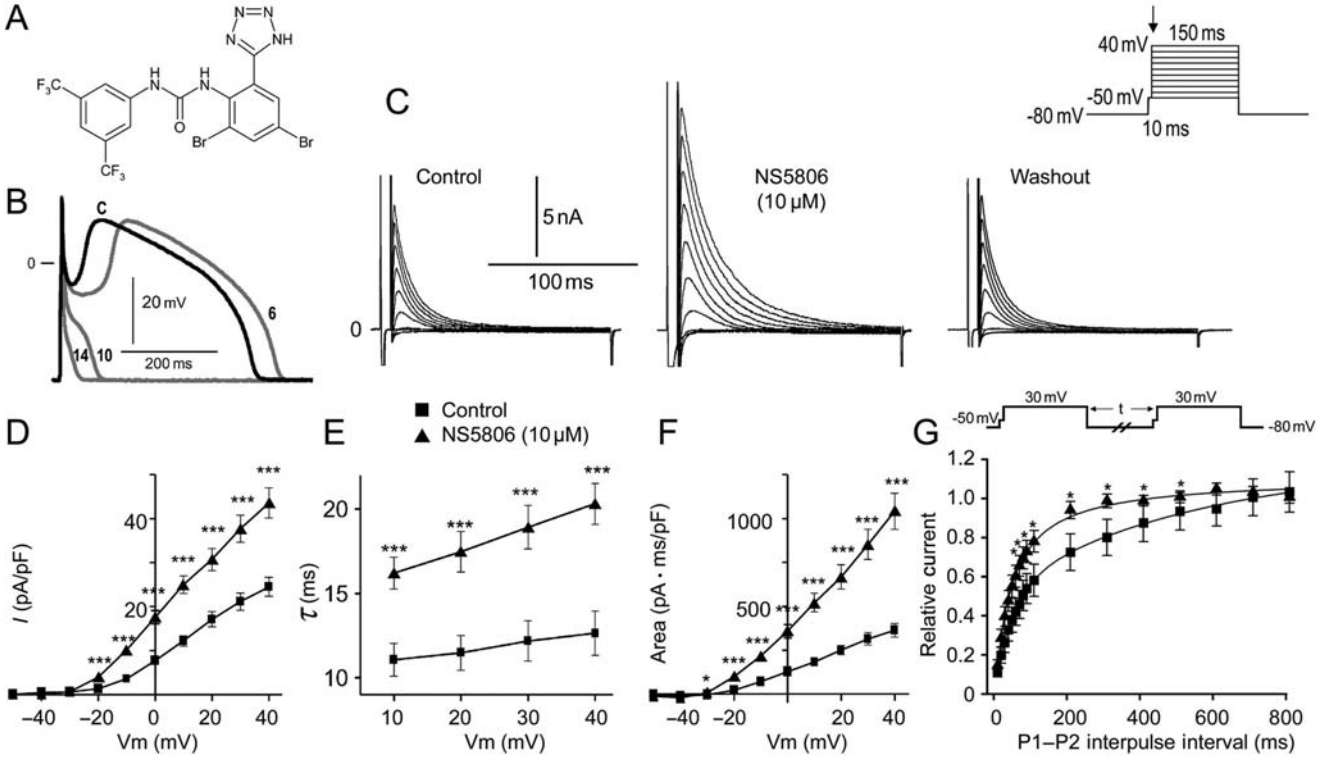

Figure 1 (*A*) Chemical structure of the diphenylurea 1-(3,5-bis-trifluoromethyl-phenyl)-3-[2,4-dibromo-6-(1H-tetrazol-5-yl)-phenyl]-urea compound, NS5806. (*B*) Action potentials recorded from a canine left ventricular (LV) mid-myocardial myocyte before (black) and at 6, 10, and 14 s after 10 μM NS5806 (grey). Basic cycle length (BCL), 1 s. Representative of $n = 5$. (*C*) Representative I_{to} recorded from isolated LV mid-myocardial myocytes in the absence and presence of 10 μM NS5806, $n = 7$. (*D*) Current–voltage (*I–V*) relation of peak I_{to} before and after 10 μM NS5806. (*E*) Time constant of decay of I_{to} before and after 10 μM NS5806. (*F*) Graph showing area under the curve, reflecting the total charge carried by I_{to}. (*G*) I_{to} recovery from inactivation using a two-pulse protocol. Statistical significance was evaluated by paired *t*-test.

direction of repolarization and a progressive inversion of the T-wave corresponding to the type 1 BrS ECG. At a concentration of 15 μM, NS5806 increased phase 1, leading to loss of the AP dome at some epicardial sites. The spike-and-dome AP morphology was maintained at other epicardial sites, resulting in an epicardial dispersion of repolarization (EDR). Conduction of the AP dome, from sites at which it was maintained to sites at which it was

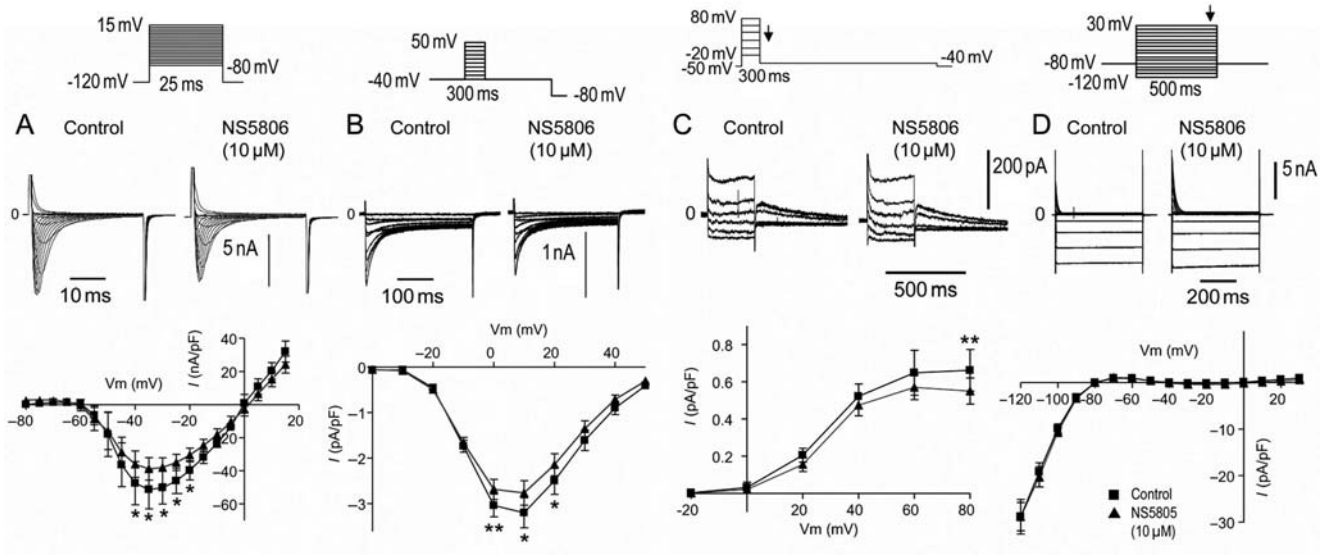

Figure 2 Effect of NS5806 on I_{Na} and I_{CaL} recorded for isolated canine left ventricular (LV) mid-myocardial cells and on I_{Kr} in endocardial LV myocytes. (*A*) Representative I_{Na} traces and average *I–V* relation recorded before and after 10 μM NS5806 ($n = 4$). (*B*) I_{CaL} was elicited by the shown protocol preceded by five pre-pulses (from −80 to +20 mV for 200 ms) to ensure constant load of the sarcoplasmic reticulum. Representative I_{CaL} traces and average *I–V* relations recorded before and after 10 μM NS5806 ($n = 6$). (*C*) Representative I_{Kr} and I_{Kr} tail currents measured at −35 mV as a function of voltage at the preceding voltage step before and after the application of 10 μM NS5806 ($n = 7$). (*D*) Representative I_{K1} recordings in mid-myocardial cells ($n = 8$) and the current–voltage relationship at the end of the step protocol before and after the application of 10 μM NS5806. Statistical significance was evaluated by paired *t*-test.

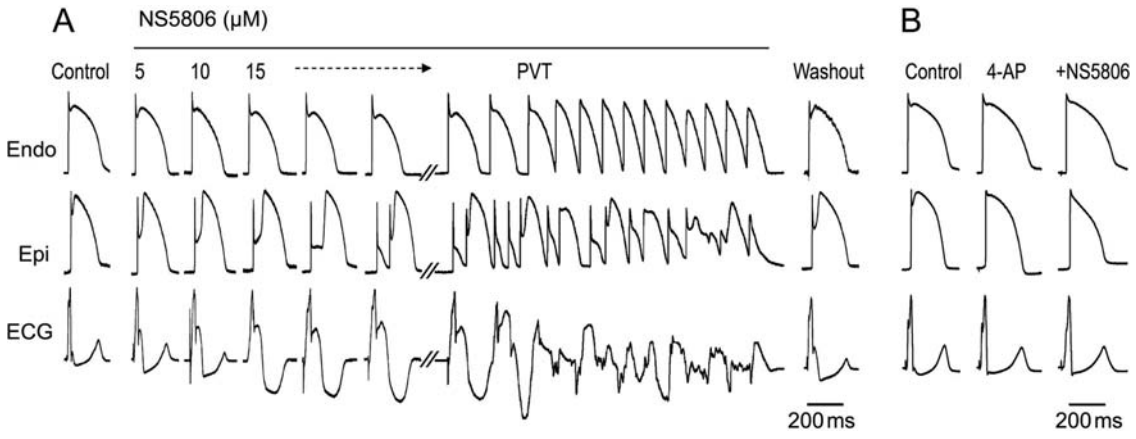

Figure 3 Effect of NS5806 to induce the electrocardiographic and arrhythmic manifestation of Brugada syndrome in a canine right ventricular wedge preparation paced from the endocardial surface at a basic cycle length of 2 s. (*A*) Endocardium and epicardium action potentials and ECG were recorded before and after 5, 10, and 15 μM NS5806, as well as after 30 min of washout. About 15 μM NS5806 induce polymorphic ventricular tachycardia (PVT). Representative of $n = 4$. (*B*) About 2 mM 4-aminopyrodine (4-AP) blocked I_{to} and prevented 10 μM NS5806 from increasing the epicardial notch in a left ventricular wedge. Representative of $n = 4$.

lost, caused local re-excitation via a phase 2 re-entry mechanism, leading to the development of closely coupled extrasystoles. The loss of the dome in the epicardium also created a transmural dispersion of repolarization (TDR) and refractoriness. The combination of EDR and TDR created a vulnerable window within the RV preparation, which when captured by a closely coupled extrasystole induced self-terminating runs of rapid PVT. These runs of PVT often deteriorated to ventricular fibrillation. Washout of the drug terminated the arrhythmia and restored AP towards control. We next investigated the effect of NS5806 in the presence of the I_{to} inhibitor, 4-aminopyrodine

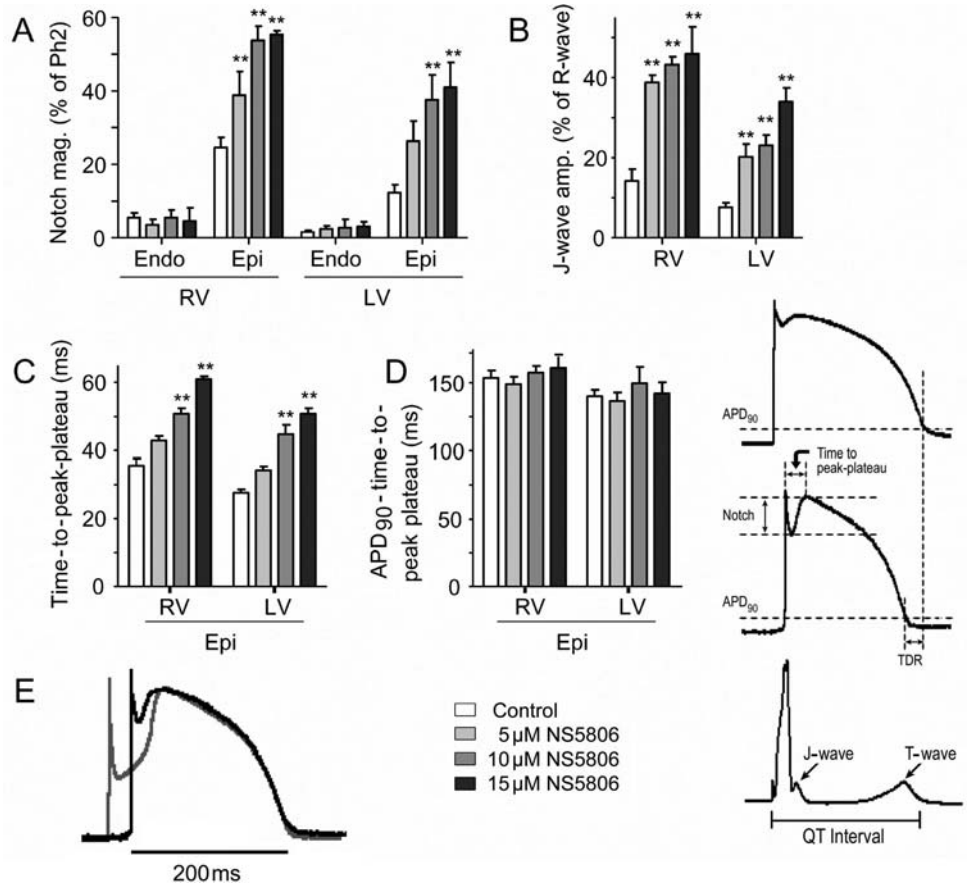

Figure 4 Effect of NS5806 on action potential (AP) parameters recorded from canine right (RV) and left ventricular (LV) wedge preparations paced at a basic cycle length of 2 s. Composite data of the effect of NS5806 (0–15 μM) on: (*A*) AP notch magnitude as percentage of the phase 2 amplitude. (*B*) J-wave amplitude as percentage of the R-wave amplitude. (*C*) Time-to-peak-plateau in epicardial APs. (*D*) Repolarization time measured as action potential duration (APD_{90}) minus time-to-peak-plateau. (*E*) Superimposed LV epicardial APs recorded in control (black trace) and after 15 μM NS5806 (grey trace). The APs were superimposed at the time of peak of phase 2 ($n = 5$–8).

(4-AP), as shown in *Figure 3B*. The application of 4-AP (2 mM) abolished the epicardial notch, and in the continued presence of 4-AP, NS5806 (10 μM) failed to enhance the epicardial notch and the J-wave on the ECG. In the presence of 4-AP and NS5806, there appeared to be some change in phase 2, which may be due to an effect on I_{CaL} (*Figure 2B*). The arrhythmias could also be terminated by introducing 4-AP (2 mM) in the continued presence of 15 μM NS5806 ($n = 4$, data not shown).

The effects of NS5806 on notch magnitude and J-wave amplitude on both LV and RV wedges are summarized in *Figure 4A* and *B*. In both RV and LV preparations, there was a concentration-dependent increase in the size of the epicardial notch, whereas the endocardium was largely unaffected. In addition to the effect on the notch, the time from the onset of the epicardial AP to the peak of phase 2 (the time-to-peak plateau) was significantly augmented by increasing concentrations of NS5806 (*Figure 4C*), whereas the repolarization time (APD_{90} minus the time-to-peak plateau) remained constant (*Figure 4D*). Superimposed traces recorded from the epicardium in the absence and presence of NS5806 illustrate that the drug effect was mainly on notch magnitude and time-to-peak plateau, whereas the time and morphology of the repolarization phase were largely unaltered (*Figure 4E*).

NS5806 prolonged epicardial APD_{90} and QT intervals in both LV and RV preparations (*Figure 5A* and *B*) and the effective refractory period increased in proportion to the increase in APD_{90} (*Table 1*). *Figure 5C* shows the interdependence of APD_{90} and notch amplitude in the epicardium, following exposure to increasing concentrations of NS5806. The prolongation of the APD_{90} was significant only in the epicardium. This differential effect on the epi- and endocardial ADP90 suggested the TDR would be affected and *Figure 5D* presents a plot of TDR under the various conditions tested. At lower concentrations of NS5806, the TDR was diminished and at 15 μM even reversed. TDR was greatest just before and after the loss of the epicardial AP dome.

The arrhythmias associated with BrS often occur at rest, whereas at higher heart rates, there is a normalization of the ECG. In agreement with these observations, we found that the epicardial notch magnitude was higher at slow rates and most pronounced in the RV wedges (*Figure 6A* and *B*). The smaller epicardial notch magnitude at 300 and 500 ms BCL pacing is due to some inactivation of I_{to} (*Figure 1G*). The application of NS5806 sped up the recovery of I_{to} (*Figure 1G*), resulting in relatively larger epicardial notch magnitudes at faster pacing in both RV and LV wedges. The BrS phenotype is also modulated by autonomic influences on the heart. The syndrome can be unmasked by vagal stimulation, whereas sympathetic stimulation is effective in preventing the ECG and arrhythmic manifestations of BrS.[19] In another series of experiments, we examined the effect of sympathetic agonists. *Figure 6C* shows representative recordings of APs from LV ventricular wedge preparations recorded under control conditions, after NS5806 (15 μM) and NS5806 (15 μM)+isoproterenol (iso, 25 nM). *Figure 6D* illustrates composite data from three experiments. Iso reversed the effects of NS5806 towards control values.

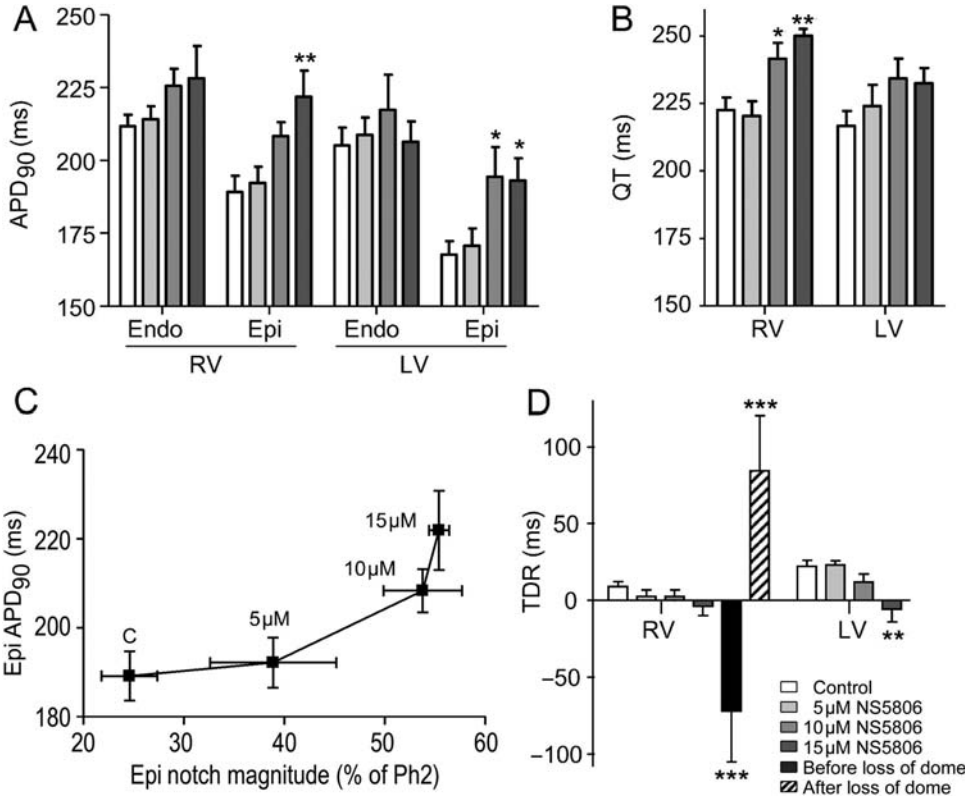

Figure 5 Effect of NS5806 (0–15 μM) on action potential duration (APD_{90}), QT interval, and transmural dispersion of repolarization (TDR) in canine right (RV) and left (LV) ventricular wedge preparations. BCL, 2 s. (*A*) APD_{90}; (*B*) QT interval; (*C*) epicardial ADP_{90} plotted as a function of epicardial notch magnitude. (*D*) TDR calculated as the time interval between repolarization of the endocardial and epicardial action potentials measured at 90%. For the RV preparations, TDR was measured just before and after the dome was lost in the presence of 15 μM NS5806. $n = 5–8$.

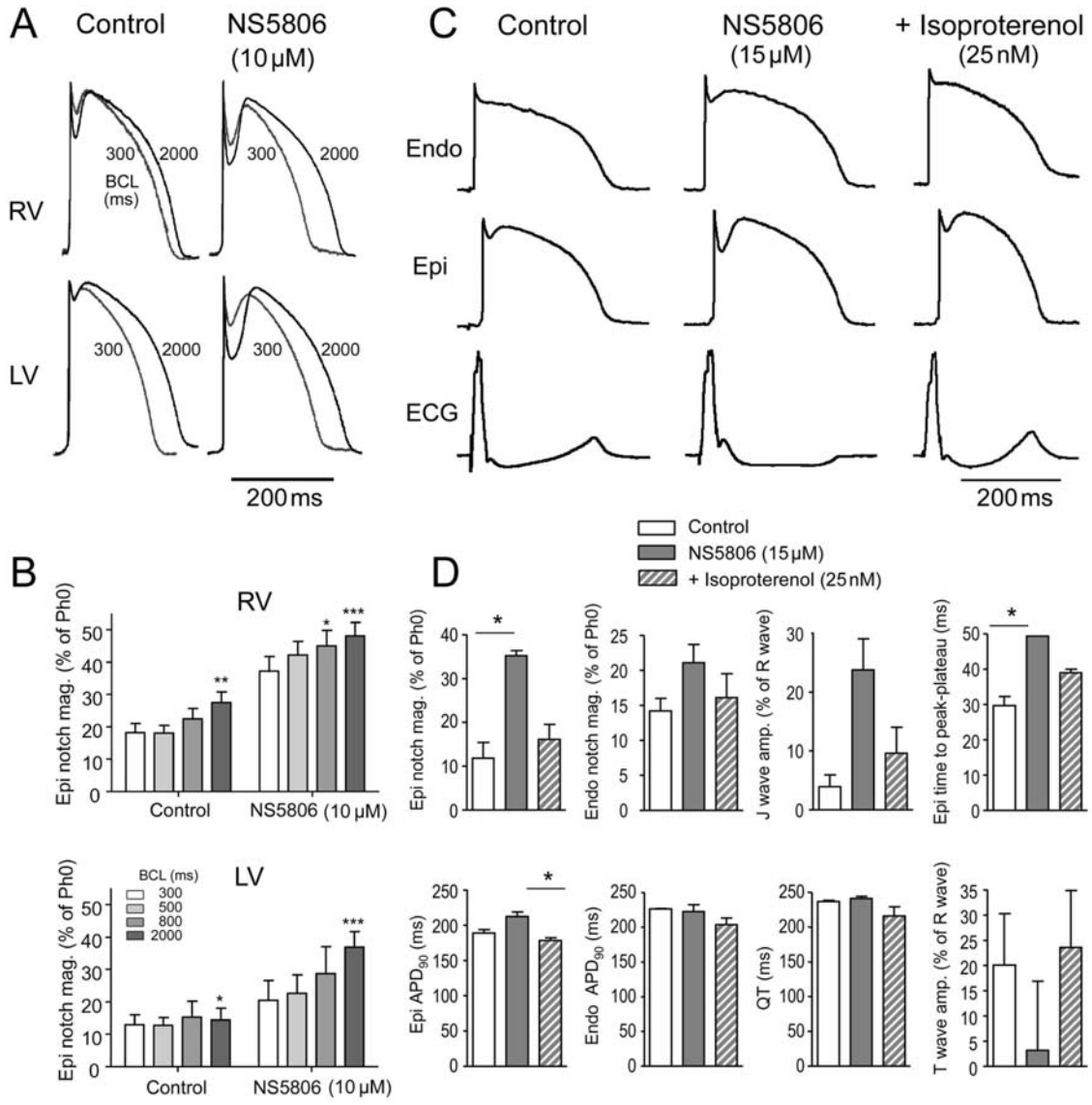

Figure 6 The effect of NS5806 (10 μM) at different pacing rates on the epicardial notch magnitude. (*A*) Representative action potentials (APs) recorded at increasing basic cycle lengths from 300 to 2000 ms from canine right (RV) and left (LV) ventricular wedge preparations. (*B*) The epicardial notch magnitude is plotted as percentage of phase 0 amplitude ($n = 4$–6). (*C*) Effect of isoproterenol (25 nM) to reverse the effect of NS5806 (15 μM) in a left ventricular wedge preparation. Representative of $n = 3$. (*D*) Mean data showing effect of NS5806 and NS5806+iso on various electrophysiological parameters. Results were compared by Friedman's test and Dunn's post-test.

Although sodium and calcium channel blockers are capable of inducing BrS only in RV wedge preparations, the I_{to} activator was able to induce the phenotype in wedges from both the RV and LV of the canine heart. *Figure 7* shows representative recordings from an LV wedge exposed to increasing concentrations of NS5806. As with RV wedge preparations, the size of the epicardial notch was progressively more accentuated with a parallel increase in the amplitude of the J wave. At a concentration of 15 μM, NS5806 induced PVT (*Figure 7B*). Two epicardial AP recordings were recorded simultaneously to demonstrate the heterogeneity in the tissue. Although PVTs were inducible in preparations from both RV and LV, the RV was more sensitive, most likely due to the higher intrinsic levels of I_{to}. At a concentration of 15 μM, NS5806 induced BrS in four of six RV wedge preparations, compared with 2 of 10 LV wedge preparations (*Figure 7C*). The depth of the epicardial notch under control conditions was an important determinant of whether or not arrhythmias would develop (*Figure 7D*).

4. Discussion

In this study, we introduce and characterize the first known I_{to} activator and use it to generate a new experimental model of BrS. The I_{to} activator NS5806 is shown to increase peak I_{to} amplitude and to delay inactivation in isolated cardiomyocytes, resulting in an accentuated phase 1 repolarization accompanied by the loss of the AP dome in mid- and epicardial cells.

A link between mutations in genes responsible for I_{to} and the development of BrS was recently reported by Delpón *et al.*,[10] in which a mutation in the *KCNE3* gene was found to be associated with the development of BrS. KCNE3 normally interacts with $K_v4.3$ to suppress I_{to}, [20] and the

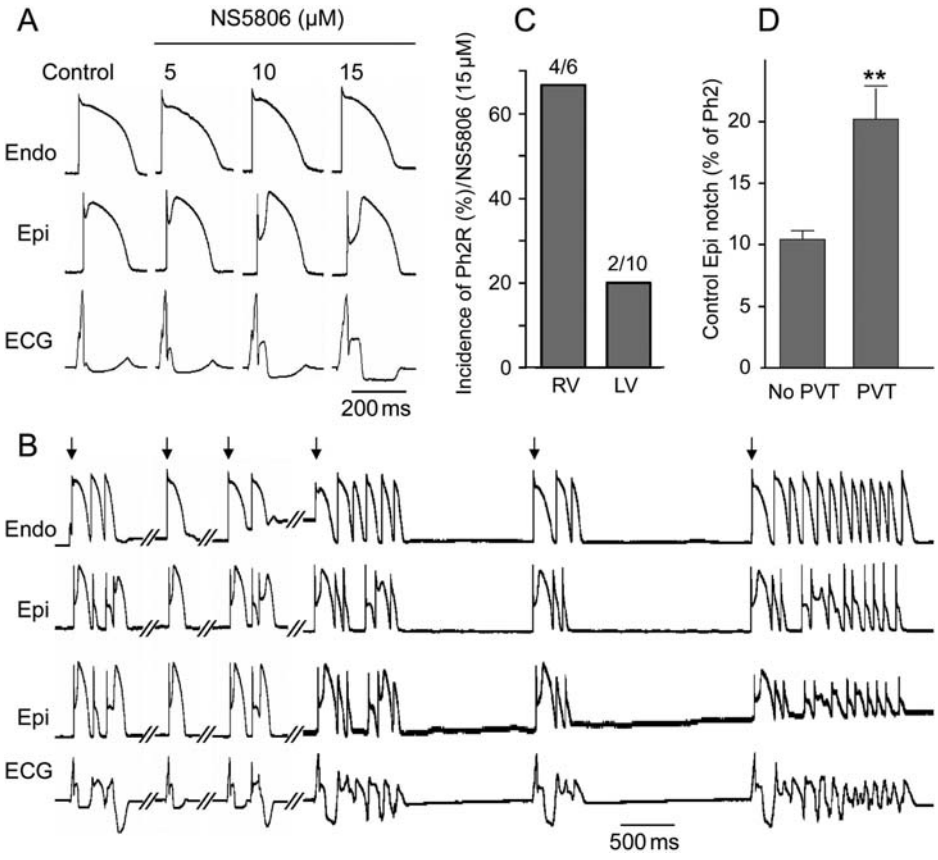

Figure 7 Effect of NS5806 to induce the electrocardiographic and arrhythmic manifestation of Brugada syndrome in a canine left ventricular (LV) wedge preparation paced at a basic cycle length of 2 s. (*A*) Representative recordings of action potentials and corresponding ECG before and after NS5806 (0–15 μM). (*B*) The same preparation following 35 min exposure to 15 μM NS5806, showing development of polymorphic ventricular tachycardia (PVT). The arrows indicate paced beats. (*C*) Incidence of PVT in the presence of 15 μM NS5806 in right ventricular (RV) wedge vs. LV wedge preparations. (*D*) Size of the epicardial notch in control in preparations exhibiting PVT ($n = 6$) vs. preparations without PVT ($n = 5$). Results from RV and LV wedge preparations are pooled.

mutation in *KCNE3* was shown to result in a gain of function in I_{to}.[10] The results of our study using the I_{to} activator are consistent with the clinical observations that an enhancement of I_{to} can lead to the development of BrS.

It is well established that mutations leading to a decrease in I_{Na} or I_{CaL} can also cause BrS in humans.[6–9] Previously developed experimental models of BrS, consistent with these genotypes, involved the use of sodium and calcium channel blockers such as terfenadine and verapamil in RV wedge preparations.[21–23] Other experimental models of BrS involved the use of $I_{K\text{-}ATP}$ activators such as pinacidil.[12] The new experimental model, involving the use of an I_{to} activator, recapitulates all the electrographic and arrhythmic manifestation of BrS, thus providing evidence in support of a pivotal role for I_{to} in the genesis of the disease.

BrS is an RV disease, in which ST-segment elevation is usually limited to the right precordial leads. The RV manifestations of the disease are thought to be due to the prominence of I_{to} in RV vs. LV epicardium.[12] Less commonly encountered is a variant of BrS, in which ST-segment elevation is present in the left or inferior leads or throughout the precordium.[3–5,24–26] Our results demonstrate for the first time the ability to induce BrS phenotype in LV tissues. NS5806 was able to induce the phenotype in wedges from both RV and LV of the canine heart, suggesting that augmentation of I_{to} could induce the BrS phenotype in any region of the heart. This suggests that a genetic defect leading to a prominent gain of function of I_{to} could explain variants of BrS, in which ST-segment elevation or J-waves are evident in right, left, or inferior ECG leads. To date, a single BrS patient carrying an SCN5A mutation exhibiting ST-elevation in the right and inferior leads has been described;[5] however, the ST elevation in the inferior leads was found in one of four family members and other gene candidates were not studied.

Arrhythmias associated with BrS are often triggered by vagal influence and bradycardia.[1] We found that in both RV and LV, the effect of NS5806 to amplify the epicardial notch magnitude was bradycardia-dependent (*Figure 6A* and *B*). Furthermore, the effect of sympathetic influences to reverse the effects of the I_{to} activator to induce the BrS phenotype (*Figure 6C* and *D*) is consistent with the ameliorative effects of β-adrenergic agonists in the clinic, in which isoproterenol has been shown to be effective in normalizing the ST-elevation and in controlling electrical storm in BrS patients.[27,28] This effect is due to the positive chronotropic effect and increased calcium current secondary to increased intracellular cAMP rather than inhibition of I_{to}.

Our new experimental model of BrS also recapitulates the clinical finding that a slight increase in QT interval is observed in the right precordial leads in association with ST-segment elevation in some BrS patients.[6] Our model shows that the prolongation of APD_{90} in the epicardium is

caused by an increase in time-to-peak plateau, following exposure to increasing concentrations of NS5806 (*Figure 5*).

In summary, our experimental model recapitulates the electrocardiographic manifestations of BrS and should prove useful in further assessment of the cellular mechanisms underlying the development of arrhythmias associated with BrS and particularly valuable in the identification of pharmacological agents useful in the approach to therapy.

Acknowledgements

The authors wish to thank Judy Hefferon and Arthur Iodice for valuable technical assistance.

Conflict of interest: R.S.H. and M.G. are employees of NeuroSearch. S.P.O. is a consultant to the company.

Funding

This work was supported by grants from the Carlsberg Foundation [2006010173 to K.C.]; the American Health Assistance Foundation [J.M.C.]; the Danish National Research Foundation [S.P.O.]; the National Institutes of Health [HL 47678 to CA] and the Masons of New York State and Florida.

References

1. Antzelevitch C. Brugada syndrome. *Pacing Clin Electrophysiol* 2006;**29**:1130–1159.
2. Brugada P, Brugada J. Right bundle branch block, persistent ST segment elevation and sudden cardiac death: a distinct clinical and electrocardiographic syndrome. A multicenter report. *J Am Coll Cardiol* 1992;**20**:1391–1396.
3. Horigome H, Shigeta O, Kuga K, Isobe T, Sakakibara Y, Yamaguchi I *et al*. Ventricular fibrillation during anesthesia in association with J waves in the left precordial leads in a child with coarctation of the aorta. *J Electrocardiol* 2003;**36**:339–343.
4. Ogawa M, Kumagai K, Yamanouchi Y, Saku K. Spontaneous onset of ventricular fibrillation in Brugada syndrome with J wave and ST-segment elevation in the inferior leads. *Heart Rhythm* 2005;**2**:97–99.
5. Potet F, Mabo P, Le CG, Probst V, Schott JJ, Airaud F *et al*. Novel Brugada SCN5A mutation leading to ST segment elevation in the inferior or the right precordial leads. *J Cardiovasc Electrophysiol* 2003;**14**:200–203.
6. Antzelevitch C, Pollevick GD, Cordeiro JM, Casis O, Sanguinetti MC, Aizawa Y *et al*. Loss-of-function mutations in the cardiac calcium channel underlie a new clinical entity characterized by ST-segment elevation, short QT intervals, and sudden cardiac death. *Circulation* 2007;**115**:442–449.
7. Chen Q, Kirsch GE, Zhang D, Brugada R, Brugada J, Brugada P *et al*. Genetic basis and molecular mechanism for idiopathic ventricular fibrillation. *Nature* 1998;**392**:293–296.
8. Watanabe H, Koopmann TT, Le SS, Yang T, Ingram CR, Schott JJ *et al*. Sodium channel beta1 subunit mutations associated with Brugada syndrome and cardiac conduction disease in humans. *J Clin Invest* 2008;**118**:2260–2268.
9. London B, Michalec M, Mehdi H, Zhu X, Kerchner L, Sanyal S *et al*. Mutation in glycerol-3-phosphate dehydrogenase 1 like gene (GPD1-L) decreases cardiac Na+ current and causes inherited arrhythmias. *Circulation* 2007;**116**:2260–2268.
10. Delpón E, Cordeiro JM, Núñez L, Bloch-Thomsen PE, Guerchicoff A, Pollevick GD *et al*. Functional effects of *KCNE3* mutation and its role in the development of Brugada syndrome. *Circ Arrhythmia Electrophysiol* 2008;**1**:209–218.
11. Di Diego JM, Sun ZQ, Antzelevitch C. I(to) and action potential notch are smaller in left vs. right canine ventricular epicardium. *Am J Physiol* 1996;**271**:H548–H561.
12. Di Diego JM, Cordeiro JM, Goodrow RJ, Fish JM, Zygmunt AC, Perez GJ *et al*. Ionic and cellular basis for the predominance of the Brugada syndrome phenotype in males. *Circulation* 2002;**106**:2004–2011.
13. Cordeiro JM, Greene L, Heilmann C, Antzelevitch D, Antzelevitch C. Transmural heterogeneity of calcium activity and mechanical function in the canine left ventricle. *Am J Physiol Heart Circ Physiol* 2004;**286**:H1471–H1479.
14. Cordeiro JM, Malone JE, Di Diego JM, Scornik FS, Aistrup GL, Antzelevitch C *et al*. Cellular and subcellular alternans in the canine left ventricle. *Am J Physiol Heart Circ Physiol* 2007;**293**:H3506–H3516.
15. Dumaine R, Cordeiro JM. Comparison of K+ currents in cardiac Purkinje cells isolated from rabbit and dog. *J Mol Cell Cardiol* 2007;**42**:378–389.
16. Cordeiro JM, Mazza M, Goodrow R, Ulahannan N, Antzelevitch C, Di Diego JM. Functionally distinct sodium channels in ventricular epicardial and endocardial cells contribute to a greater sensitivity of epicardium to electrical depression. *Am J Physiol Heart Circ Physiol* 2008;**295**:H154–H162.
17. Verkerk AO, Wilders R, Schulze-Bahr E, Beekman L, Bhuiyan ZA, Bertrand J *et al*. Role of sequence variations in the human ether-a-go-go-related gene (HERG, KCNH2) in the Brugada syndrome. *Cardiovasc Res* 2005;**68**:441–453.
18. Gordon E, Lozinskaya IM, Lin Z, Semus SF, Blaney FE, Willette RN *et al*. PD-307243 causes instantaneous current through human ether-a-go-go-related gene (hERG) potassium channels. *Mol Pharmacol* 2007;**73**:639–651.
19. Antzelevitch C, Fish JM. Therapy for the Brugada syndrome. *Handb Exp Pharmacol* 2006;305–330.
20. Lundby A, Olesen SP. KCNE3 is an inhibitory subunit of the Kv4.3 potassium channel. *Biochem Biophys Res Commun* 2006;**346**:958–967.
21. Fish JM, Antzelevitch C. Role of sodium and calcium channel block in unmasking the Brugada syndrome. *Heart Rhythm* 2004;**1**:210–217.
22. Yan GX, Antzelevitch C. Cellular basis for the Brugada syndrome and other mechanisms of arrhythmogenesis associated with ST-segment elevation. *Circulation* 1999;**100**:1660–1666.
23. Aiba T, Shimizu W, Hidaka I, Uemura K, Noda T, Zheng C *et al*. Cellular basis for trigger and maintenance of ventricular fibrillation in the Brugada syndrome model: high-resolution optical mapping study. *J Am Coll Cardiol* 2006;**47**:2074–2085.
24. Kalla H, Yan GX, Marinchak R. Ventricular fibrillation in a patient with prominent J (Osborn) waves and ST segment elevation in the inferior electrocardiographic leads: a Brugada syndrome variant? *J Cardiovasc Electrophysiol* 2000;**11**:95–98.
25. Ogawa R, Kishi R, Mihara K, Takahashi H, Takagi A, Matsumoto N *et al*. Population pharmacokinetic and pharmacodynamic analysis of a class IC antiarrhythmic, pilsicainide, in patients with cardiac arrhythmias. *J Clin Pharmacol* 2006;**46**:59–68.
26. Ozeke O, Aras D, Celenk MK, Deveci B, Yildiz A, Topaloglu S *et al*. Exercise-induced ventricular tachycardia associated with J point ST-segment elevation in inferior leads in a patient without apparent heart disease: a variant form of Brugada syndrome? *J Electrocardiol* 2006;**39**:409–412.
27. Suzuki H, Torigoe K, Numata O, Yazaki S. Infant case with a malignant form of Brugada syndrome. *J Cardiovasc Electrophysiol* 2000;**11**:1277–1280.
28. Tanaka H, Kinoshita O, Uchikawa S, Kasai H, Nakamura M, Izawa A *et al*. Successful prevention of recurrent ventricular fibrillation by intravenous isoproterenol in a patient with Brugada syndrome. *Pacing Clin Electrophysiol* 2001;**24**:1293–1294.